

Mutually interacting tachyon dark energy with variable G and Λ

Jafar Sadeghi¹, Martiros Khurshudyan², Margarit Hakobyan^{3,4} and Hoda Farahani¹

¹ Department of Physics, Faculty of Basic Sciences, University of Mazandaran, P. O. Box 47416-95447, Babolsar, Iran; *pouriya@ipm.ir*; *h.farahani@umz.ac.ir*

² Max Planck Institute of Colloids and Interfaces, Potsdam-Golm Science Park Am Mhlenberg 1 OT Golm 14476 Potsdam, Germany; *martiros.khurshudyan@nano.cnr.it*

³ A.I. Alikhanyan National Science Laboratory, Alikhanian Brothers St., Yerevan, Armenia; *margarit@mail.yerphi.am*

⁴ Department of Nuclear Physics, Yerevan State University, Yerevan, Armenia

Received 2014 March 3; accepted 2014 May 18

Abstract We consider a tachyonic scalar field as a model of dark energy with interaction between components in the case of variable G and Λ . We assume a flat Universe with a specific form of scale factor and study cosmological parameters numerically and graphically. Statefinder analysis is also performed. For a particular choice of interaction parameters we succeed in obtaining an analytical expression of densities. We find that our model will be stable at the late stage but there is an instability in the early Universe, so we propose this model as a realistic model of our Universe.

Key words: cosmology — early universe — cosmological parameters — dark energy

1 INTRODUCTION

In order to explain recent observational data, which reveal accelerating expansion of the Universe, several models have been proposed. One of the possible scenarios is the existence of a dark energy with negative pressure and positive energy density adding an acceleration to the expansion.

Various kinds of dark energy model have been proposed, such as cosmological constant (Peebles & Ratra 2003), quintessence (Ratra & Peebles 1988; Caldwell et al. 1998; Sami & Padmanabhan 2003), k-essence (Armendariz-Picon et al. 2001; Chiba 2002; Scherrer 2004), tachyon (Sen 2002a,b; Gibbons 2002; Sadeghi et al. 2014a), phantom (Caldwell 2002; Elizalde et al. 2004; Cline et al. 2004), ghost dark energy (Sadeghi et al. 2013b; Feng et al. 2012a,b, 2013), Chaplygin gas and its extensions (Kamenshchik et al. 2001; Amani & Pourhassan 2013; Sadeghi et al. 2013a; Khurshudyan 2013; Saadat & Pourhassan 2013a,b,c, 2014; Sadeghi & Farahani 2013; Pourhassan 2013), quintom (Feng et al. 2006), holographic dark energy (Hořava & Minic 2000; Sadeghi et al. 2014b; Setare & Jamil 2010; Aghamohammadi et al. 2011; Durán et al. 2010), and extra dimensions (Rogatko 2004; Amani & Pourhassan 2012).

Among the above models concerning the nature of the dark component of the Universe, in this article, we assume that it could be described by a scalar field and we choose a scalar field called the tachyonic field with the following relativistic Lagrangian

$$L_{TF} = -V(\phi)\sqrt{1 - \partial_\mu\phi\partial^\mu\phi}, \quad (1)$$

which has attracted a lot of attention (see, for instance, references in Verma & Pathak 2012). The stress energy tensor is given by

$$T^{ij} = \frac{\partial L_{\text{TF}}}{\partial(\partial_i \phi)} \partial^j \phi - g^{ij} L_{\text{TF}}, \quad (2)$$

which defines the energy density and pressure as the following expressions

$$\rho = \frac{V(\phi)}{\sqrt{1 - \partial_i \phi \partial^i \phi}}, \quad (3)$$

and,

$$P = -V(\phi) \sqrt{1 - \partial_i \phi \partial^i \phi}. \quad (4)$$

Our next step is to decompose Equations (3) and (4) as

$$\begin{aligned} \rho &= \rho_m + \rho_\Lambda, \\ P &= P_m + P_\Lambda, \end{aligned} \quad (5)$$

with the following components:

$$\begin{aligned} \rho_m &= \frac{V(\phi) \partial_i \phi \partial^i \phi}{\sqrt{1 - \partial_i \phi \partial^i \phi}}, \\ P_m &= 0, \\ \omega_m &= 0, \end{aligned} \quad (6)$$

and

$$\begin{aligned} \rho_\Lambda &= V(\phi) \sqrt{1 - \partial_i \phi \partial^i \phi}, \\ P_\Lambda &= -V(\phi) \sqrt{1 - \partial_i \phi \partial^i \phi}, \\ \omega_\Lambda &= -1. \end{aligned} \quad (7)$$

This means that we can consider the tachyonic scalar field to be a combination of a cosmological constant and pressureless matter with $\omega_m = 0$. From a mathematical point of view, this is not the only possibility and a different splitting could be considered.

We should note that a flat FRW metric with the line element

$$ds^2 = dt^2 - a(t)^2 (dr^2 + r^2 d\theta^2 + r^2 \sin^2 \theta d\phi^2) \quad (8)$$

will be used for our purposes.

Recently, Verma & Pathak (2012) considered a model where the components of a tachyonic scalar field mutually interact. Motivated by the idea presented in that work, we would like to consider the interaction $Q = 3Hb\rho + \gamma\dot{\rho}$ in the general form between components in the case of variable G and Λ . As is well known, the Einstein equation has two important parameters which are the gravitational constant G and the cosmological constant Λ . It is known that G plays the role of a coupling constant between geometry and matter in the Einstein equations. In an evolving Universe, it appears natural to look at this constant as a function of time (Tiwari 2009; Jamil & Debnath 2011). Also, a time-dependent cosmological constant has been considered by several works in various variable G theories (Banerjee et al. 1985; Abdussattar & Vishwakarma 1997). It is possible to point out a boundary on G ; for instance, observation of the spinning-down rate of pulsar PSRJ 2019+2425 provides the result

$$\left| \frac{\dot{G}}{G} \right| \leq (1.4 - 3.2) \times 10^{-11} \text{ yr}^{-1}. \quad (9)$$

From observations of the pulsating white dwarf star G 117–B15A, the asteroseismological bound may be (Biesiada & Malec 2004)

$$\left| \frac{\dot{G}}{G} \right| \leq 4.1 \times 10^{-10} \text{ yr}^{-1}. \quad (10)$$

Today, Λ has an incredibly small value, $\Lambda < 10^{-46} \text{ GeV}^4$, whereas generic inflation models require that Λ has a large value during the inflationary epoch. This is the source of the cosmological constant problem. We hope that consideration of variable Λ could solve this problem. Also, a pioneering work on varying cosmological constant and its interaction with matter suggested how to resolve the fine-tuning problem (Wang & Meng 2005). Therefore, we apply these ideas to the recent work (Verma & Pathak 2012) and extend this model.

Also, interacting models may solve the cosmic coincidence problem (del Campo et al. 2009; He et al. 2011). He et al. (2010) find that the interaction between dark sectors cannot ensure that the dark energy fully clusters along with dark matter. There are several possibilities to choose an interaction term, for example those introduced by Chen et al. (2011). It is also possible to construct a holographic cosmological model where dark matter and dark energy interact non-gravitationally with each other (Durán & Pavón 2011). In the interesting work by Xu et al. (2013), the effects of interaction between dark matter and dark energy on the evolution of the gravitational and the peculiar velocity fields were investigated. In a recent work (Costa et al. 2013), it was concluded that an interaction is compatible with recent observations and can provide a strong argument towards consistency of different values of cosmological parameters. All of these give us motivation to use interaction to produce a comprehensive model.

This paper is organized as follows. In Section 2 we will introduce the equations which govern our model. Then, in Section 3, we study statefinder diagnostics. In Section 4, we will consider the mathematics and solution strategy of the problem for the non-interacting case and will present an analysis of the model for a special type of scale factor. The model including interaction between components will also be analyzed numerically and cosmological parameters discussed graphically. Section 5 includes discussion and the conclusions.

2 THE FIELD EQUATIONS

The field equations that govern our model with variable $G(t)$ and $\Lambda(t)$ (see for instance Abdussattar & Vishwakarma 1997) are

$$H^2 = \frac{\dot{a}^2}{a^2} = \frac{8\pi G(t)\rho}{3} + \frac{\Lambda(t)}{3}, \quad (11)$$

and

$$\frac{\ddot{a}}{a} = -\frac{4\pi G(t)}{3}(\rho + 3P) + \frac{\Lambda(t)}{3}. \quad (12)$$

The energy density (3) and pressure (4) of a tachyonic field are reduced to the following expressions

$$\rho = \frac{V(\phi)}{\sqrt{1 - \dot{\phi}^2}}, \quad (13)$$

and

$$P = -V(\phi)\sqrt{1 - \dot{\phi}^2}. \quad (14)$$

Also, the energy conservation $T_{ij}^{;j} = 0$ reads

$$\dot{\rho} + 3H(\rho + P) = 0. \quad (15)$$

In the case of conservation of particle number in the Universe, the combination of (11), (12) and (15) gives the following relationship between $\dot{G}(t)$ and $\dot{\Lambda}(t)$

$$\dot{G} = -\frac{\dot{\Lambda}}{8\pi\rho}. \quad (16)$$

Hereafter, we will assume special forms of scale factor $a(t)$ and cosmological constant $\Lambda(t)$. This assumption allows us to determine $G(t)$, ρ , ϕ and $V(\phi)$. Before investigation of these quantities we study statefinder diagnostics.

3 STATEFINDER DIAGNOSTICS

In the framework of general relativity it is accepted that dark energy can explain the present cosmic acceleration. Besides the cosmological constant, there are many other candidates for dark energy. The property of dark energy is model dependent, and to differentiate different models of dark energy a sensitive diagnostic tool is needed.

The Hubble parameter H and deceleration parameter q are very important quantities, which can describe the geometric properties of the Universe. Since $\dot{a} > 0$, $H > 0$ implies there is expansion of the Universe. Also, $\ddot{a} > 0$, i.e. $q < 0$, indicates there is accelerated expansion of the Universe. Since the various dark energy models give $H > 0$ and $q < 0$, they cannot provide enough evidence to identify which more general models of dark energy are supported by more accurate cosmological observational data. For this aim we need a higher order of time derivative for the scale factor and geometrical tool. Sahni et al. (2003) proposed a geometrical statefinder diagnostic tool, based on dimensionless parameters (r, s) , which are functions of the scale factor and its time derivative. These parameters are defined as

$$r = \frac{1}{H^3} \frac{\ddot{a}}{a}, \quad (17)$$

and

$$s = \frac{r - 1}{3(q - \frac{1}{2})}, \quad (18)$$

where the deceleration parameter is given by

$$q = -\frac{1}{H^2} \frac{\ddot{a}}{a}. \quad (19)$$

This can be rewritten as the following

$$q = \frac{1}{2} \left(1 + 3 \frac{8\pi G(t)P_\Lambda - \Lambda(t)}{8\pi G(t)\rho + \Lambda(t)} \right). \quad (20)$$

We provide a numerical description of statefinder parameters in the next section.

4 METHOD

In this paper we use the following forms of scale factor, cosmological constant and interaction term.

We assume that the Universe is in a quasi-exponential expansion phase with the following scale factor (Verma & Pathak 2012)

$$a(t) = a_0 t^n \exp(\alpha t). \quad (21)$$

We also assume the following scale factor-dependent cosmological constant

$$\Lambda(t) = H^2 + Aa^{-k}. \quad (22)$$

Finally, we consider the following interaction term

$$Q = 3Hb\rho + \gamma\dot{\rho}. \quad (23)$$

In the $\gamma = 0$ limit, the interaction term is reduced to what is used in, for example, Izquierdo & Pavón (2010); Ferreira et al. (2013). There are undetermined constants n, α, A, k, b , and γ in Equations (21)–(23), which will be fixed in our numerical study. We have already discussed the forms and types of interaction Q at length in our previous works (Sadeghi et al. 2013a,b; Khurshudyan 2013). We just mention to our readers concerning the form considered in this article that it carries a phenomenological aspect $\gamma\dot{\rho}$, introduced from a unit correctness point of view. This form will be one of the forms intensively considered in the literature from different perspectives and found to be suitable for cosmological problems. Generally in the literature, many authors are taking such terms, which will simplify the problem and will have analytical solutions.

In this case, we obtain the following equation, which describes the dynamics of G

$$\dot{G} + \frac{(Akt^2 + 2n(a_0e^{\alpha t}t^n)^k)(n + \alpha t)}{At^3 - 2t(a_0e^{\alpha t}t^n)^k(n + \alpha t)^2}G = 0. \quad (24)$$

The absence of an interaction between components means that components evolve separately, i.e. Equation (15) separates into the following equations

$$\dot{\rho}_m + 3H(\rho_m + P_m) = 0, \quad (25)$$

and

$$\dot{\rho}_\Lambda + 3H(\rho_\Lambda + P_\Lambda) = 0. \quad (26)$$

From Equation (22), for the energy density of tachyonic matter, we obtain

$$\rho_m = \rho_{0m}e^{[-3(\alpha t + n \ln t)]}. \quad (27)$$

For the pressure of a cosmological constant P_Λ we have

$$P_\Lambda = \rho_{0m}e^{[-3(\alpha t + n \ln t)]} + \frac{A(a_0t^n e^{\alpha t})^{-k} - 2t^{-2}(n + \alpha t)}{8\pi G}. \quad (28)$$

For the tachyonic field and potential we obtain

$$\phi(t) = \int \sqrt{1 - \frac{8\pi G\rho_\Lambda}{2t^{-2}(n + \alpha t)^2 - A(a_0t^n e^{\alpha t})^{-k}}} dt, \quad (29)$$

and

$$V(\phi) = \frac{\rho_\Lambda}{\sqrt{1 - \dot{\phi}^2}}, \quad (30)$$

where $\rho_\Lambda = -P_\Lambda$ is used. This means that $\dot{\phi}^2 \leq 1$. In the special case of $\dot{\phi}^2 = 1$, the tachyon potential diverges and takes an infinite value.

On the other hand, accounting for interaction between cosmic components modifies (25) and (26) in such a way that the conservation of energy holds. In this case we have

$$\dot{\rho}_m + 3H(\rho_m + P_m) = Q, \quad (31)$$

and

$$\dot{\rho}_\Lambda + 3H(\rho_\Lambda + P_\Lambda) = -Q. \quad (32)$$

Therefore, corresponding to our case with $\omega_m = 0$ and $\omega_\Lambda = -1$, we can obtain

$$(1 - \gamma)\dot{\rho}_m + 3H(1 - b)\rho_m = 3Hb\rho_\Lambda + \gamma\dot{\rho}_\Lambda, \quad (33)$$

and

$$(1 + \gamma)\dot{\rho}_\Lambda + 3Hb\rho_\Lambda = -3Hb\rho_m - \gamma\dot{\rho}_m. \quad (34)$$

We use the above relations to generate a numerical analysis for our system to understand the behavior of some important cosmological parameters.

4.1 Analytical Results

Before performing numerical analysis of some important cosmological parameters in the general case, we try to obtain time-dependent densities and pressures in the special case where we restrict interaction parameters such that $b = \gamma$. This assumption helps us to decouple equations given by (33) and (34) to extract $\rho_\Lambda(t)$ and $\rho_m(t)$. Then, by using relations (31) and (32) we can obtain the pressure $P_\Lambda(t)$. In this case, we can also investigate the stability of the theory (see discussion section).

Under the above assumption we can obtain the following densities

$$\rho_\Lambda = ct^{-3n\gamma^3} e^{-3\alpha\gamma^3 t}, \quad (35)$$

and

$$\rho_m = ct^{-3n} e^{-3\alpha t} \left[1 - \frac{\gamma^3 + \gamma^2 - 1}{\gamma^3 - 1} t^{3n(1-\gamma^3)} e^{-3\alpha(\gamma-1)(\gamma^2+\gamma+1)t} \right], \quad (36)$$

where c is a constant of integration. These lead to the following pressure

$$P_\Lambda = \frac{c(\gamma^6 - \gamma^5 - 2\gamma^3 + \gamma^2 + 1)}{\gamma^3 - 1} t^{-3n\gamma^3} e^{-3\alpha\gamma^3 t}. \quad (37)$$

Therefore, we can write the following expression for total density

$$\rho = c \left[t^{-3n\gamma^3} e^{-3\alpha\gamma^3 t} + \left(1 - \frac{\gamma^3 + \gamma^2 - 1}{\gamma^3 - 1} t^{-3n\gamma(\gamma^3-1)} e^{-3\alpha(\gamma-1)(\gamma^2+\gamma+1)t} \right) t^{-3n} e^{-3\alpha t} \right]. \quad (38)$$

As we expected, $P_m = 0$. Therefore, from Equations (28) and (37) one can obtain

$$8\pi G = \frac{t^{n(3\lambda^3+2)} e^{\alpha t(3\lambda^3+2)} - 2t^{3n\lambda^3+3n-2} e^{3\alpha t(\lambda^3+1)} n - 2t^{3n\lambda^3+3n-1} e^{3\alpha t(\lambda^3+1)} \alpha}{c\lambda^3 e^{3\alpha t} t^{3n} - c\lambda^2 e^{3\alpha t} t^{3n} - t^{3n\lambda^3} e^{3\alpha\lambda^3 t} - ce^{3\alpha t} t^{3n}}. \quad (39)$$

4.2 Numerical Results

In this section, we numerically solve equations from the previous sections and obtain the potential and field, behavior of $G(t)$, deceleration parameter q , and total equation of state, which is given by

$$\omega_{\text{tot}} = \frac{P_m + P_\Lambda}{\rho_m + \rho_\Lambda}, \quad (40)$$

which, for the case of $P_m = 0$, reduces to the following form

$$\omega_{\text{tot}} = \frac{P_\Lambda}{\rho_m + \rho_\Lambda}. \quad (41)$$

The reader should remember that $\omega_{\text{tot}} \neq \omega_1 + \omega_2$. By using the scale factor given by Equation (21), the Hubble parameter H is reduced to the following relation

$$H = \frac{n}{t} + \alpha, \quad (42)$$

and the cosmological constant (22) takes the following form

$$\Lambda(t) = A(a_0 \exp[\alpha t] t^n)^{-k} + \frac{(n + \alpha t)^2}{t^2}. \quad (43)$$

Below, we graphically present the behavior of G , q and ω_{tot} . All parameters are fixed in order to obtain $V \rightarrow 0$ when $t \rightarrow \infty$.

First of all, we consider the non-interacting case and plot $G(t)$, $\omega_{\text{tot}}(t)$ and $q(t)$ for some fixed parameters in Figures 1, 2 and 3 respectively. Then, in Figures 4, 5 and 6 we obtain the behavior of these quantities in the presence of the interaction term given by Equation (23).

In the next step, we plot ϕ , V and P_Λ in terms of time for the non-interacting case in Figures 7, 8 and 9 respectively. Then, extension to the interacting case is illustrated in Figures 10, 11, 12, 13 and 14, where ρ_m and ρ_Λ are also analyzed.

All figures contain four plots with different fixed parameters. First, in the case of the non-interacting component, the first plot (top, left) is drawn for $n = 3$, $\alpha = 0.5$, $k = 1.5$ and different values of A . The second plot (top, right) is drawn for $n = 3$, $k = 1.5$, $A = 2.5$ and different values of α . The third plot (bottom, left) is drawn for $n = 3$, $\alpha = 0.5$, $A = 2.5$ and different values of k . Finally, the fourth plot (bottom, right) is drawn for $k = 1.5$, $\alpha = 0.5$, $A = 0.5$ and different values of n .

On the other hand, in the case of interacting components, the first plot (top, left) is drawn for $A = 1$, $\alpha = 1.1$, $\gamma = 0.05$, $k = 0.5$, $b = 0.04$ and different values of n . The second plot (top, right) is drawn for $n = 2.5$, $k = 0.5$, $A = 1$, $\gamma = 0.05$, $b = 0.04$ and different values of α . The third plot (bottom, left) is drawn for $n = 1.5$, $\alpha = 2.5$, $A = 1.5$, $k = 1.5$, $\gamma = 0.05$ and different values of b . Finally, the fourth plot (bottom, right) is drawn for $k = 1.5$, $\alpha = 2.5$, $A = 1.5$, $n = 1.5$, $b = 0.04$ and different values of γ .

In Figure 15 we graphically study statefinder parameters. Also in Figure 16, stability of the theory is investigated. In the next section, we provide a discussion about these figures and effects of parameters on the cosmological quantities.

5 DISCUSSION AND CONCLUSIONS

In this paper, we considered mutually interacting tachyon dark energy and extended it to the case of variable G and Λ . We obtained behavior of some cosmological quantities by using analytical and numerical analysis. Under some assumptions we obtained analytical expressions for energy densities in terms of time, which allow us to obtain the tensor to scalar ratio. We fixed some parameters to unity and reduced the number of free parameters in the models. We found that higher values of n are in more agreement with observational data.

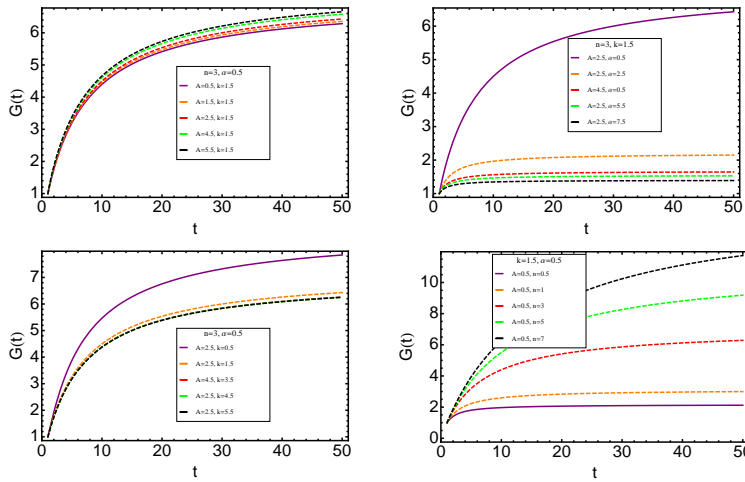


Fig. 1 Behavior of G vs. t for non-interacting components where we choose $a_0 = 2$ and $\rho_0 = 1$.

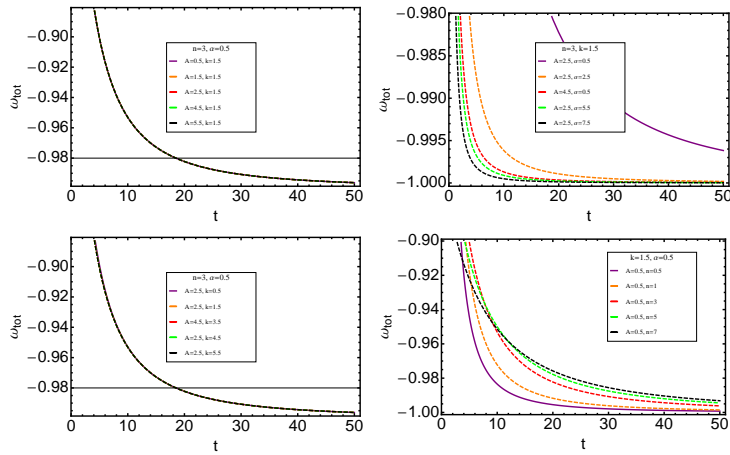


Fig. 2 Behavior of ω_{tot} vs. t for non-interacting components where we choose $a_0 = 2$ and $\rho_0 = 1$.

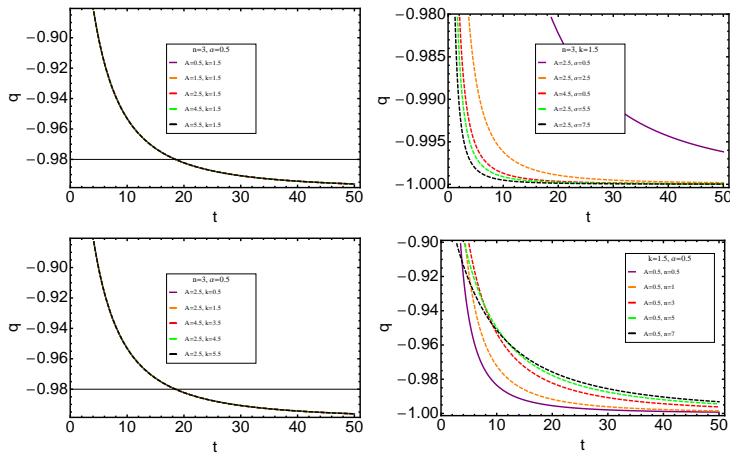


Fig. 3 Behavior of q vs. t for non-interacting components where we choose $a_0 = 2$ and $\rho_0 = 1$.

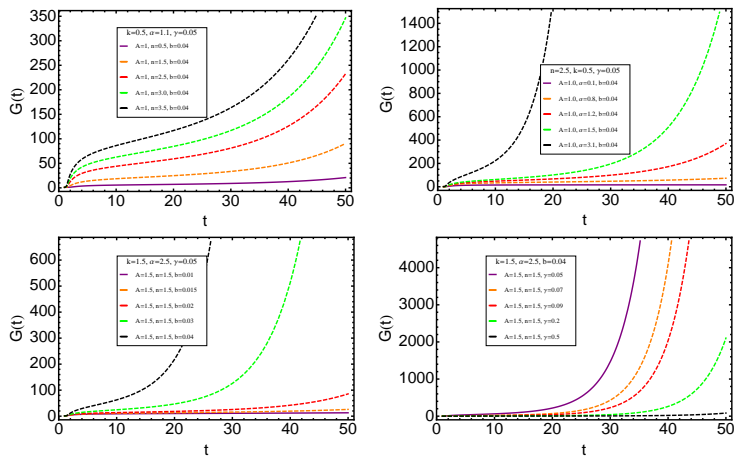


Fig. 4 Behavior of $G(t)$ vs. t for interacting components where we choose $a_0 = 1$.

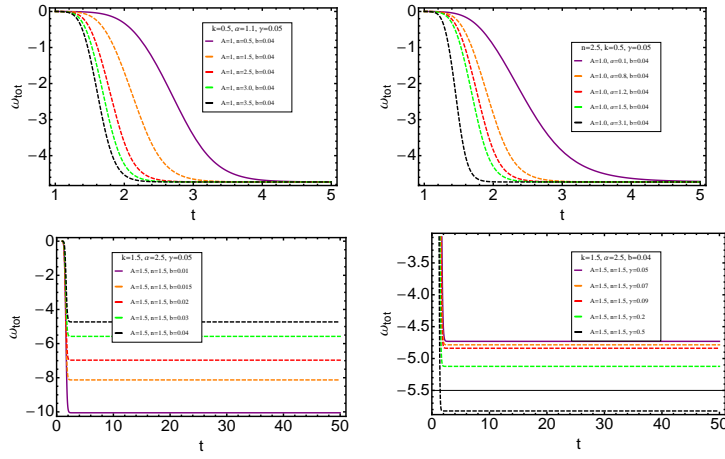


Fig. 5 Behavior of ω_{tot} vs. t for interacting components where we choose $a_0 = 1$.

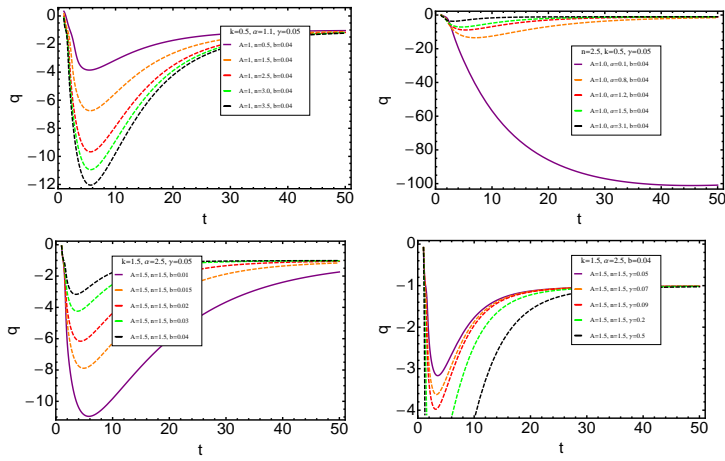


Fig. 6 Behavior of q vs. t for interacting components where we choose $a_0 = 1$.

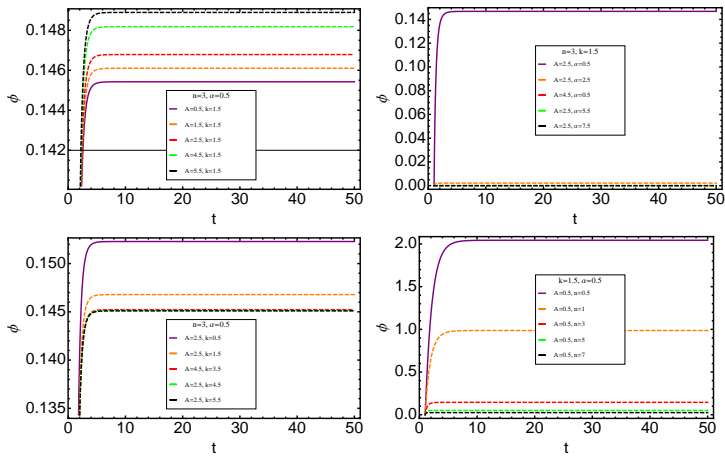


Fig. 7 Behavior of ϕ vs. t for non-interacting components where we choose $a_0 = 2$ and $\rho_0 = 1$.

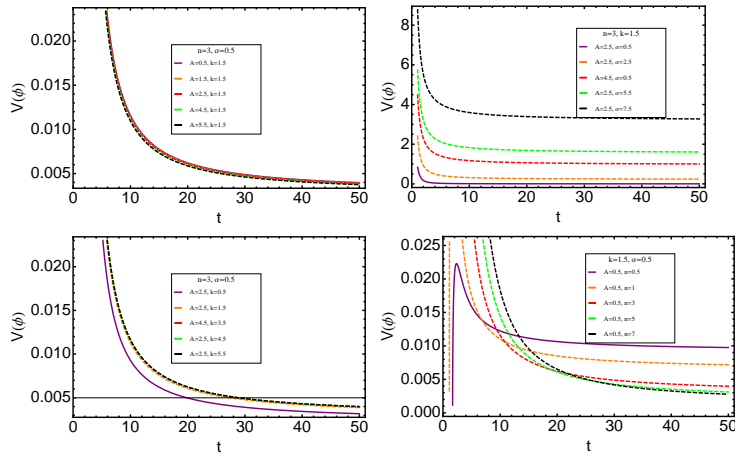


Fig. 8 Behavior of V vs. t for non-interacting components where we choose $a_0 = 2$ and $\rho_0 = 1$.

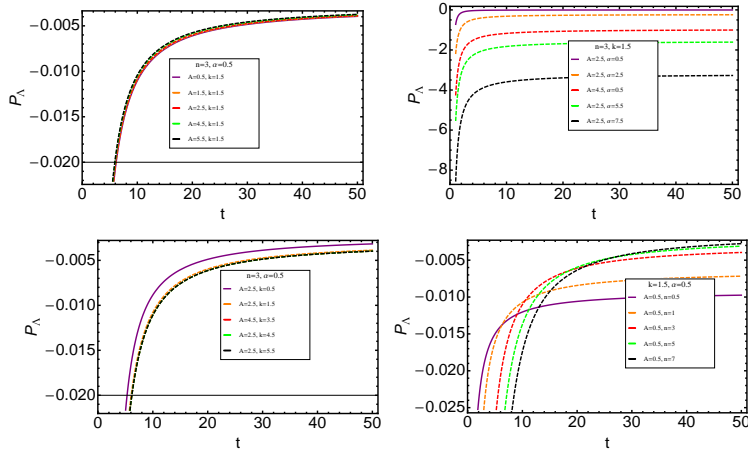


Fig. 9 Behavior of P_Λ vs. t for non-interacting components where we choose $a_0 = 2$ and $\rho_0 = 1$.

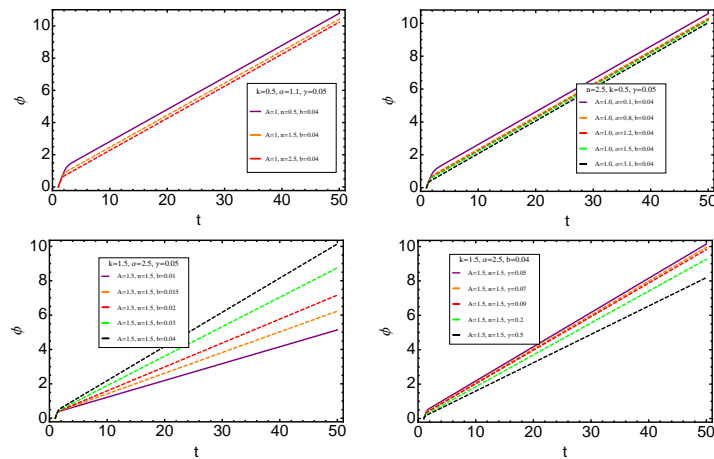


Fig. 10 Behavior of ϕ vs. t for interacting components where we choose $a_0 = 1$.

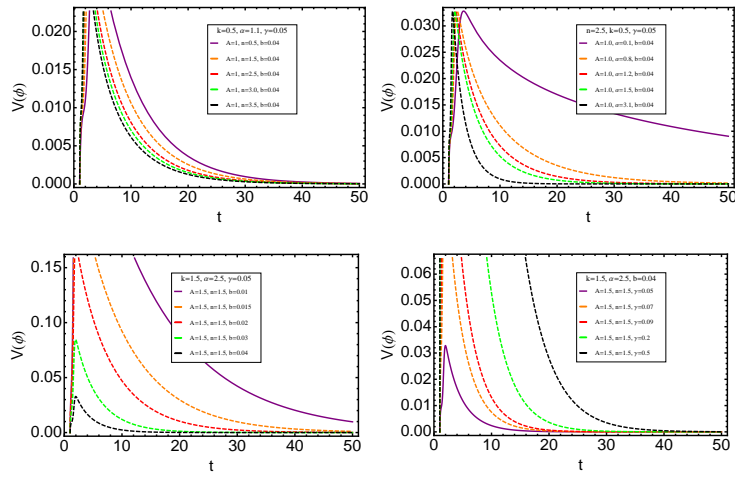


Fig. 11 Behavior of V vs. t for interacting components where we choose $a_0 = 1$.

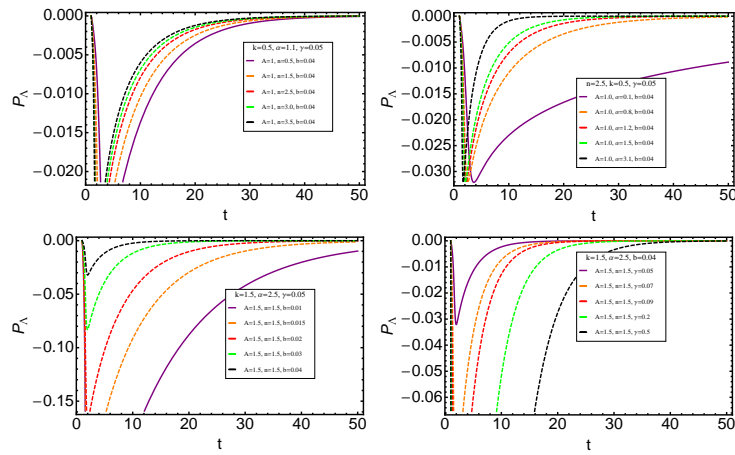


Fig. 12 Behavior of P_Λ vs. t for interacting components where we choose $a_0 = 1$.

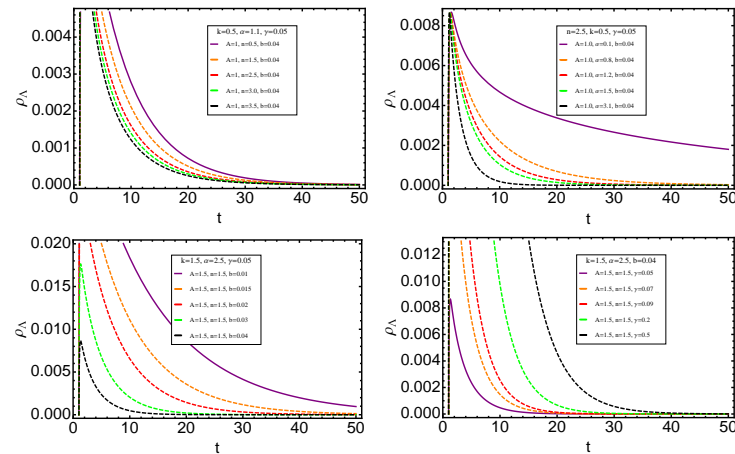


Fig. 13 Behavior of ρ_Λ vs. t for interacting components where we choose $a_0 = 1$.

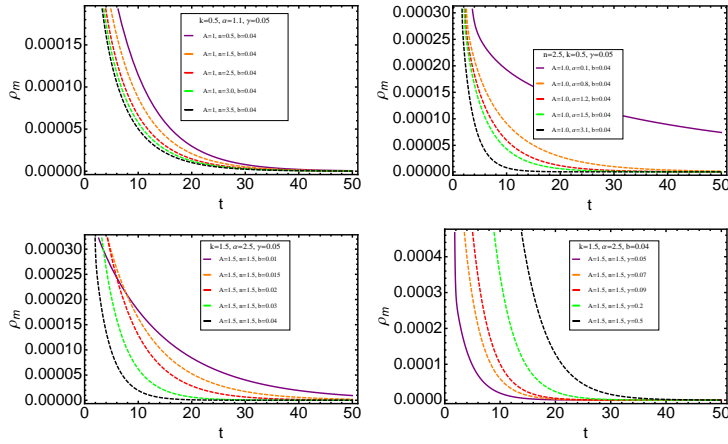


Fig. 14 Behavior of ρ_m vs. t for interacting components where we choose $a_0 = 1$.

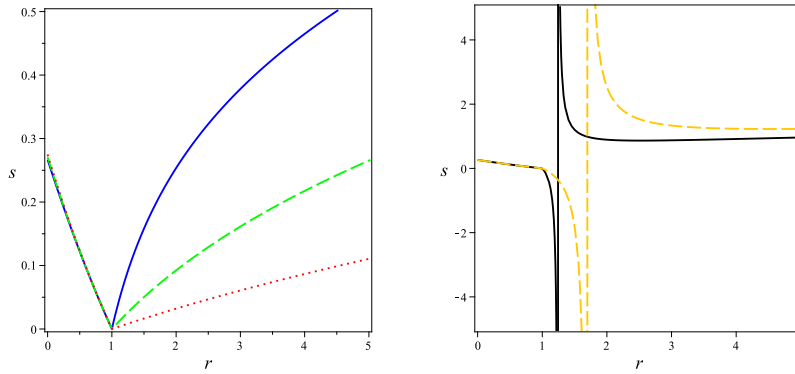


Fig. 15 Behavior of s vs. r by choosing $a_0 = 1$. Left: $n = 1$ (solid line), $n = 2$ (dashed line) and $n = 5$ (dotted line). Right: $n = 0.6$ (solid line) and $n = 0.5$ (dashed line).

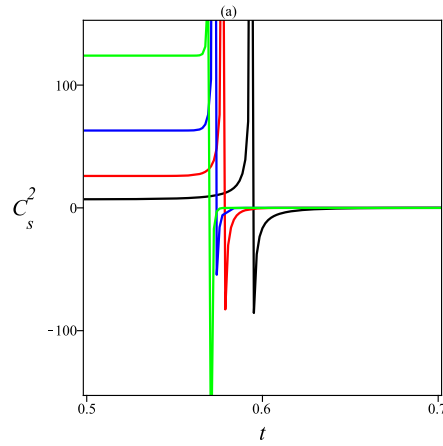


Fig. 16 Behavior of C_s^2 vs. r , for $n = 1$ and $\alpha = 1$. $b = \gamma = 2$ (black), $b = \gamma = 3$ (red), $b = \gamma = 4$ (blue) and $b = \gamma = 5$ (green).

Below, we give two steps to explain cosmological quantities which were numerically obtained. In the first step we deal with $G(t)$, $\omega_{\text{tot}}(t)$ and q , and in the second step we deal with $\phi(t)$, V , P_Λ , ρ_Λ and ρ_m . In the first step we are able to compare our results with observational data, but in the second step there is no measurement of the parameters.

Plots of Figure 1 show behavior of G versus t with variation of A , α , n and k . We found that G is an increasing function of t at the early step, which yields a constant in the later step. It is clear from Figure 1 that increasing A and n increases the value of G , but increasing α and k decreases the value of G .

Plots in Figure 2 show the behavior of ω_{tot} versus t with variation of A , α , n and k . We found that ω_{tot} is totally negative after the initial time which yields -1 at large t . It is clear from Figure 2 that increasing the parameter n increases the value of ω_{tot} , but increasing α decreases the value of ω_{tot} . We also found that variation of A and k has no important effect on ω_{tot} . The black line in the last plot, which corresponds to $n = 7$, illustrates the opposite behavior at the early stage which is more expected, therefore, we can restrict this parameter as $n > 6$.

Plots in Figure 3 show behavior of the declaration parameter q versus t with variation of A , α , n and k . We found that q is totally negative after the initial time which corresponds to accelerating expansion of the Universe. Also, it yields -1 after large time which suggests there is a constant value for the Hubble expansion parameter and agrees with current data. It is clear from Figure 3 that increasing n increases the value of q , but increasing α decreases the value of q , and variation of A and k has no important effect on q . The current observation of $q \approx -0.8$ indicates $t \approx 2$ at the current time.

Plots in Figure 4 should be compared with those in Figure 1 to find the effect of interaction on $G(t)$. In Figure 4, we vary n , α , b and γ . We find that G is an increasing function of t at the early step, which is similar to the non-interacting case. Then, at the large stage, relating to the value of parameters, it may yield a constant or may diverge. For example, by choosing $A = 1$, $0.1 \leq \alpha \leq 0.8$, $b = 0.04$, $n = 2.5$, $k = 0.5$ and $\gamma = 0.05$ as well as $A = 1.5$, $\alpha = 2.5$, $b = 0.01$, $n = 1.5$, $k = 1.5$ and $\gamma = 0.05$, we obtain a constant G . It is clear from Figure 4 that increasing α , b and n increases the value of G , but increasing γ decreases the value of G . We can see that variation of G with α is completely different from the case of non-interacting components where, as illustrated in Figure 1, α decreases the value of G . At the current stage ($t \approx 2$), the value of G is infinitesimal, which is in agreement with current observations.

Plots in Figure 5 show behavior of ω_{tot} versus t with variation of n , α , b and γ for the case of interacting components. We found that ω_{tot} is totally negative and increasing after initial time, and yields a negative constant at large t . It is clear from Figure 5 that increasing b increases the value of ω_{tot} , but increasing α , n and γ decreases the value of ω_{tot} . We can conclude that choosing $b = 0.04$, $\gamma = 0.05$, $A = k = n = 1.5$ and $\alpha = 0.5$ gives $\omega_{\text{tot}} \rightarrow -1$.

Plots in Figure 6 show behavior of the declaration parameter q versus t for the case of interacting components. We find that q is totally negative which confirms accelerating expansion of the Universe as well as the non-interacting case. We found that this parameter decreases with time in the initial stage to reach a minimum, then increases with time to reach a constant value at the late stage which is near -1 . It is clear from Figure 6 that increasing b and α increases the value of q , but increasing n and γ decreases the value of q , which are different from the non-interacting case. It is illustrated that $q \approx -0.8$ agrees with the current stage at about $t = 2$.

Now, we consider the second set of quantities. Figures 7, 8 and 9 correspond to the non-interacting case. Plots in Figure 7 show that the scalar field ϕ increases at the initial stage and then suddenly yields a constant. So, it seems that the scalar field is constant at present. In other words, the scalar field ϕ grows suddenly and reaches the stable phase at present. This means that the tachyon field is unstable at the early stage. We find that ϕ increases with A but decreases with n , k and α . These plots suggest $0 < \alpha \leq 2$ is necessary to obtain a non-trivial scalar field.

Plots in Figure 8 show behavior of the tachyon potential versus the cosmic time which initially increases but is a decreasing function at the late stage. This is clear from the last plot which is obtained for $k = 1.5$, $\alpha = 0.5$, $A = 0.5$ and $0.5 \leq n \leq 7$. The maximum value of potential, which is obtained at the initial stage, shows that the tachyon field is unstable in the early stages of evolution. This may be because of some irreversible processes such as particle creation and annihilation. However, more analysis and studies are needed in order to verify the correct physics. We also find that increasing A and α decreases the value of potential.

Pressure from the cosmological constant for the case of the non-interacting component is illustrated in the plots in Figure 9. As expected, pressure from the cosmological constant is negative and a decreasing function of time. The second and third plots in Figure 9 show that α and k decrease the value of cosmological constant pressure, respectively. It is illustrated that the pressure from the cosmological constant diverges at the initial stage. This infinite negative pressure corresponds to a sudden expansion of the early Universe.

Plots in Figure 10 show that scalar field ϕ is a totally increasing function of time in the case of interacting components. The first and second plots suggest that increasing n and α decreases the value of the scalar field, which is similar to the non-interacting case, however there is no difference between them at the initial stage. The last two plots represent the effect of interaction terms. It is clear that b increases while γ decreases the value of the scalar field.

Tachyon potential of the interaction case is illustrated in the plots in Figure 11, which is similar to the non-interacting case. We see a transition from an unstable to a stable state at the initial stage. We find that n , α and b decrease the value of tachyon potential but γ increases the value of tachyon potential. As we expect, the tachyon potential vanishes at late time.

Plots in Figure 12 correspond to time evolution of cosmological constant pressure which is negative during time. In contrast to the non-interacting case, we see that the cosmological constant pressure increases at the initial stage to a negative minimum and then increases to zero at the late stage. We can see that n and b decrease pressure but γ increases it.

The cosmological constant density, represented by plots in Figure 13, show that it increases at the initial stage and is decreasing until now, which is in agreement with the present accelerating expansion of the Universe. It is found that n , α and b decrease the value of time-dependent density but γ increases it.

Density of pressureless matter in the presence of the interaction term is plotted in Figure 14 which is a decreasing function of time and yields an infinitesimal value at late time as expected. We found that n and α decrease the value of density but γ increases it. Variation of density with b depends on its value, so small values of b increase density but a value larger than $b = 0.02$ decreases it.

Results for statefinder parameters ($s - r$) for our model are illustrated in Figure 15. We draw a diagram for various values of n and see that the fixed point of standard Λ CDM is ($s = 0, r = 0$) for all n . For $r \geq 1$ we find that increasing n decreases s , but in the range $r \leq 1$ there is no difference between curves with different n . Also, we see different behaviors for $n > 1$ and $0 < n < 1$ in the range $r > 1$.

Finally, we can obtain suitable conditions to have a stable model. Our numerical analysis shows that the square of sound speed $C_s^2 = \dot{P}/\dot{\rho}$ is always a positive constant for $\gamma = 1$ and $b > \gamma$. Therefore, our model will be stable during evolution of the Universe. In the special case of interaction parameters discussed in Section 4 ($\gamma = b$), there are also stable regions which are illustrated in Figure 16. We can see that there are small regions in the early Universe where $C_s^2 < 0$ and our model is unstable. These regions correspond to the maximum of potential in Figure 11 which is discussed above and interpreted as a transition from an unstable to a stable state. Therefore, we obtained effects of variable G and Λ on the model, which was suggested as a model of our Universe. In summary, we proposed interacting tachyon dark energy with variable G and Λ as a toy model of our Universe which is closest to the real case.

Acknowledgements Martiros Khurshudyan has been supported by EU funds in the frame of the program FP7-Marie Curie Initial Training Network INDEX NO. 289968.

References

- Abdussattar, & Vishwakarma, R. G. 1997, *Classical and Quantum Gravity*, 14, 945
- Aghamohammadi, A., Saaidi, K., & Setare, M. 2011, *Astrophysics and Space Science*, 332, 503
- Amani, A., & Pourhassan, B. 2012, *International Journal of Theoretical Physics*, 51, 49
- Amani, A., & Pourhassan, B. 2013, *International Journal of Theoretical Physics*, 52, 1309
- Armendariz-Picon, C., Mukhanov, V., & Steinhardt, P. J. 2001, *Physical Review D*, 63, 103510
- Banerjee, A., Duttachoudhury, S. B., & Banerjee, N. 1985, *Phys. Rev. D*, 32, 3096
- Biesiada, M., & Malec, B. 2004, *MNRAS*, 350, 644
- Caldwell, R. R. 2002, *Physics Letters B*, 545, 23
- Caldwell, R. R., Dave, R., & Steinhardt, P. J. 1998, *Physical Review Letters*, 80, 1582
- Chen, X., Wang, B., Pan, N., & Gong, Y. 2011, *Physics Letters B*, 695, 30
- Chiba, T. 2002, *Physical Review D*, 66, 063514
- Cline, J. M., Jeon, S., & Moore, G. D. 2004, *Physical Review D*, 70, 043543
- Costa, A. A., Xu, X.-D., Wang, B., Ferreira, E. G. M., & Abdalla, E. 2013, arXiv:1311.7380
- del Campo, S., Herrera, R., & Pavón, D. 2009, *J. Cosmol. Astropart. Phys.*, 1, 020
- Durán, I., & Pavón, D. 2011, *Physical Review D*, 83, 023504
- Durán, I., Pavón, D., & Zimdahl, W. 2010, *J. Cosmol. Astropart. Phys.*, 7, 018
- Elizalde, E., Nojiri, S., & Odintsov, S. D. 2004, *Physical Review D*, 70, 043539
- Feng, B., Li, M., Piao, Y.-S., & Zhang, X. 2006, *Physics Letters B*, 634, 101
- Feng, C.-J., Li, X.-Z., & Shen, X.-Y. 2012a, *Modern Physics Letters A*, 27, 1250182
- Feng, C.-J., Li, X.-Z., & Xi, P. 2012b, *Journal of High Energy Physics*, 5, 46
- Feng, C.-J., Li, X.-Z., & Shen, X.-Y. 2013, *Phys. Rev. D*, 87, 023006
- Ferreira, P. C., Pavón, D., & Carvalho, J. C. 2013, *Physical Review D*, 88, 083503
- Gibbons, G. W. 2002, *Physics Letters B*, 537, 1
- He, J.-H., Wang, B., Abdalla, E., & Pavon, D. 2010, *Journal of Cosmology and Astroparticle Physics*, 12, 022
- He, J.-H., Wang, B., & Abdalla, E. 2011, *Physical Review D*, 83, 063515
- Hořava, P., & Minic, D. 2000, *Physical Review Letters*, 85, 1610
- Izquierdo, G., & Pavón, D. 2010, *Physics Letters B*, 688, 115
- Jamil, M., & Debnath, U. 2011, *International Journal of Theoretical Physics*, 50, 1602
- Kamenshchik, A., Moschella, U., & Pasquier, V. 2001, *Physics Letters B*, 511, 265
- Khurshudyan, M. 2013, arXiv:1301.1021
- Peebles, P. J. E., & Ratra, B. 2003, *Reviews of Modern Physics*, 75, 559
- Pourhassan, B. 2013, *International Journal of Modern Physics D*, 22, 1350061
- Ratra, B., & Peebles, P. J. 1988, *Physical Review D*, 37, 3406
- Rogatko, M. 2004, *Phys. Rev. D*, 70, 044023
- Saadat, H., & Pourhassan, B. 2013a, *Astrophysics and Space Science*, 343, 783
- Saadat, H., & Pourhassan, B. 2013b, *Astrophysics and Space Science*, 344, 237
- Saadat, H., & Pourhassan, B. 2013c, *International Journal of Theoretical Physics*, 52, 3712
- Saadat, H., & Pourhassan, B. 2014, *International Journal of Theoretical Physics*, 53, 1168
- Sadeghi, J., & Farahani, H. 2013, *Astrophysics and Space Science*, 347, 209
- Sadeghi, J., Khurshudyan, M., & Farahani, H. 2013a, arXiv:1308.1819
- Sadeghi, J., Khurshudyan, M., Movsisyan, A., & Farahani, H. 2013b, *J. Cosmol. Astropart. Phys.*, 12, 031
- Sadeghi, J., Khurshudyan, M., Hakobyan, M., & Farahani, H. 2014a, *International Journal of Theoretical Physics* (arXiv: 1308.5364)
- Sadeghi, J., Pourhassan, B., & Moghaddam, Z. A. 2014b, *International Journal of Theoretical Physics*, 53, 125

- Sahni, V., Saini, T. D., Starobinsky, A. A., & Alam, U. 2003, *Journal of Experimental and Theoretical Physics Letters*, 77, 201
- Sami, M., & Padmanabhan, T. 2003, *Physical Review D*, 67, 083509
- Scherrer, R. J. 2004, *Physical review letters*, 93, 011301
- Sen, A. 2002a, *Journal of High Energy Physics*, 4, 048
- Sen, A. 2002b, *Journal of High Energy Physics*, 10, 003
- Setare, M., & Jamil, M. 2010, *EPL (Europhysics Letters)*, 92, 49003
- Tiwari, R. K. 2009, *Ap&SS*, 321, 147
- Verma, M. M., & Pathak, S. D. 2012, *International Journal of Theoretical Physics*, 51, 2370
- Wang, P., & Meng, X.-H. 2005, *Classical and Quantum Gravity*, 22, 283
- Xu, X.-D., Wang, B., Zhang, P., & Atrio-Barandela, F. 2013, *Journal of Cosmology and Astroparticle Physics*, 12, 001